Supporting Information

Designing Wide-Spectrum-Responsive Cathode Catalysts with Abundant Active Sites for High-Performance Photo-Enabled Lithium-Oxygen Batteries via Band Engineering

Yanhui Gan[a,#], Min Yue[a,#], Yujia Niu[a], Chengjie Wu[a], Songtao Zhang[d], Mengtao Ma[a], Hao Gong[*a], Hairong Xue [*b,c] and Renzhi Ma[*e]

[a] Department of Chemistry and Materials Science, College of Science, Nanjing Forestry University, Nanjing 210037, P. R. China.

[b] Zhongyuan Critical Metals Laboratory, Zhengzhou University, Zhengzhou, 450001, P. R. China.

[c] State Key Laboratory of Critical Metals Beneficiation, Metallurgy and Purification, Zhengzhou 450001, P. R. China.

[d] Testing Center, Yangzhou University, Yangzhou 225009, P. R. China.

[e] Research Center for Materials Nanoarchitectonics, National Institute for Materials Science (NIMS), 1-1 Namiki, Tsukuba, Ibaraki 305-0044, Japan.

E-mail: Hao GONG, gonghao@njfu.edu.cn;

Hairong XUE, xuehairong@zzu.edu.cn;

Renzhi MA, MA.Renzhi@nims.go.jp

Materials and instrumentation

N, N-Dimethylformamide (DMF), zincnitrate, 2,3,6,7,10,11-hexahydroxytriphenylene (HHTP), hexamethylenetetramine, ethanol, acetone, isopropanol (2-Propanol), concentrated nitric acid, tetraethylene glycol dimethyl ether (TEGDME), lithium bis (trifluoromethanesulfonyl) imide (LiTFSI), Carbon nanotubes (CNT) were purchased from TanFeng Technology Co. The lithium foil was purchased from China Energy Lithium Co., Ltd. (Tianjin, China).

Powder X-ray diffraction (XRD, Rigaku D-Max 2550) with Cu Kα radiation was employed for phase identification. The morphology of the samples was examined by a JEOL JSM-6700F scanning electron microscope (SEM) and a high-resolution transmission electron microscopy (HRTEM, a JEM-2200FS electron microscope). The UV−vis spectra were performed with a U-4100 UV−vis spectrometer under the diffuse-reflection model using an integrating sphere (UV 2401/2, Shimadzu). X-ray photoelectron spectroscopy (XPS) was carried out on an ESCAlab 2201XL spectrometer. The time-resolved photoluminescence (PL) delay was recorded on a FS5 spectrophotometer under the excitation of 320 nm. Mott–Schottky curves were obtained at 2000 Hz in a CS310M electrochemical workstation. The TGA 209 F3 type thermogravimetric analyzer was used to monitor the changes in the sample's mass with temperature and time during the heating process.

Pretreatment of carbon textile

The cut carbon textile (2 * 5 cm^2) was placed in a reaction kettle. Concentrated nitric acid and water were mixed at a ratio of 1:3 and added to the kettle. The activation treatment was conducted at 140°C for 2 h. After the reaction, the carbon textile was rinsed with water until the washing solution became neutral. Subsequently, it was dried in a vacuum drying oven at 60°C for 24 h for standby.

Synthesis of ZnO seed layer

The activated carbon textile was immersed in an ethanol solution containing 5 mM $Zn(acac)_2 \cdot 2H_2O$ for 10 s, then removed and dried on a hot plate at 100°C for 5 min. This immersion-drying cycle was repeated ten times.

Synthesis of Zn-HHTP@ZnO

An aqueous solution containing 50 mM $Zn(NO_3)_2$ and 50 mM hexamethylenetetramine (HMTA) was prepared and transferred into a 30 mL glass pressure tube. The carbon textile pre-coated with ZnO seed layer was vertically immersed into the solution. The hydrothermal reaction was carried out at 85°C for 24 h. After the reaction, the sample was rinsed thoroughly and dried. Subsequently, the carbon textile was calcined in a tube furnace at 350°C for 2 h under air atmosphere with a heating rate of 5°C min-1, yielding well-aligned ZnO nanorod arrays. The as-prepared ZnO arrays were immersed in a 3 mM HHTP solution using a mixed solvent of DMF/H_2O (volume ratio 1:10). The reaction was conducted at 60°C for 30 min. After rinsing with fresh solvent, the product was vacuum-dried for further use.

Preparation of cathode and assembly of battery

Zn-HHTP@ZnO and self-supported ZnO samples were cut into 1*1 cm^2 pieces and directly used as cathodes. The photoenhanced LOBs was assembled in a self-designed quartz glass cell with metal Li as the anod and glass fiber as the separator. The assembling process was performed in a glovebox in a pure Ar atmosphere ($H_2O < 0.01$ ppm, $O_2 < 0.01$ ppm). The electrodes were immersed in 1.0 M lithium bis (trifluoromethanesulfonyl) imide (LiTFSI) in tetraethylene glycol dimethyl ether (TEGDME). The assembled battery has quartz glass windows with a diameter of 40 mm for light illumination. During the electrochemical measurements, the cell was purged with O_2 (99.999%) and the results were recorded using the CT2001A LAND Battery Test System. The active area of each sample for light illumination was maintained at 0.5 cm^2. A 300 W Xenon lamp equipped with an AM 1.5G filter was used as the light source.

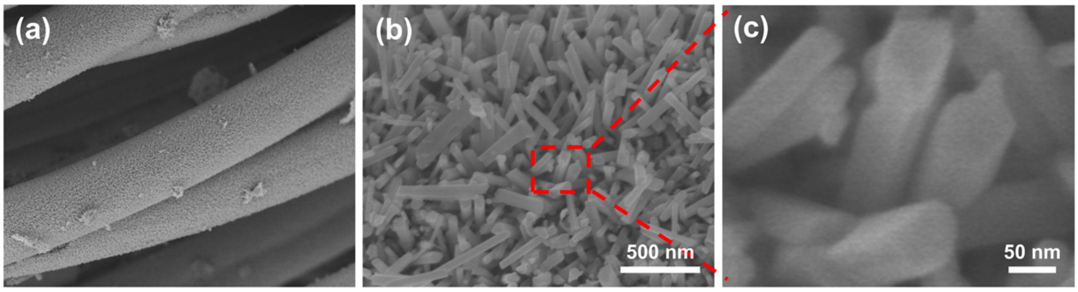

Fig. S1 SEM images of (a). Zn-HHTP@ZnO and (b-c). ZnO

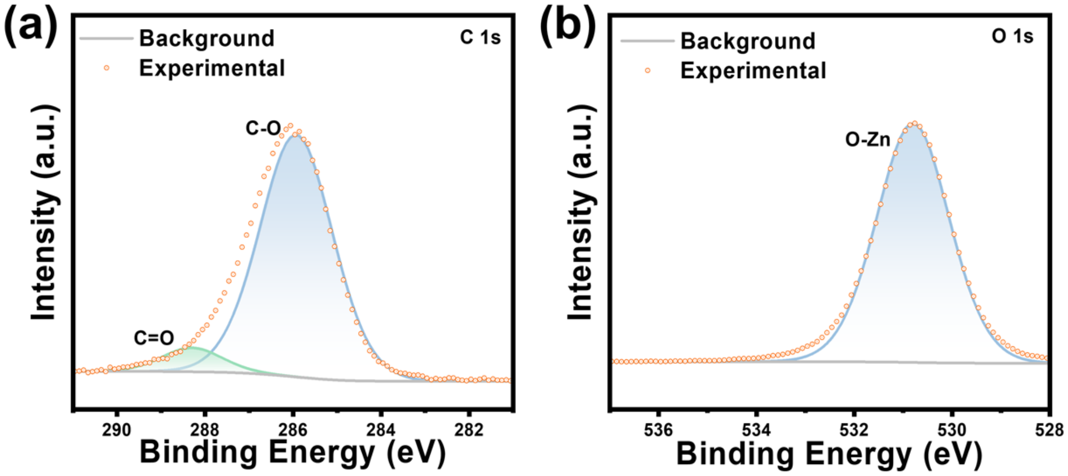

Fig. S2 (a-b) C 1s and O 1s spectrum of ZnO

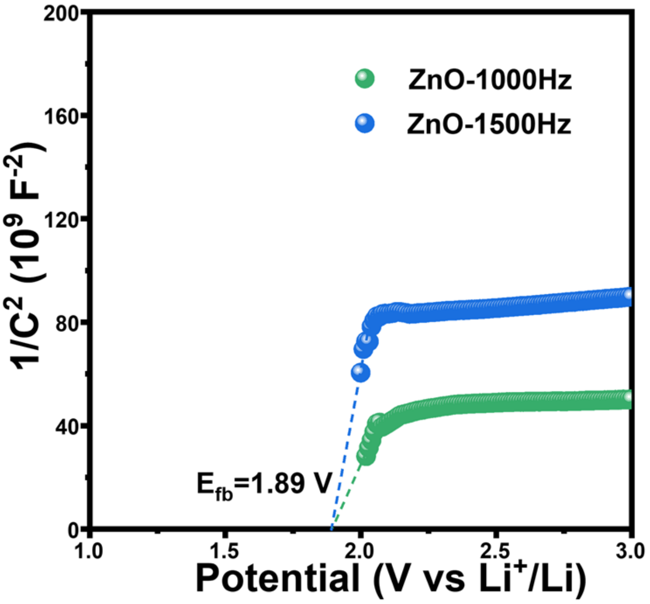

Fig. S3 Mott-Schottky curves of ZnO

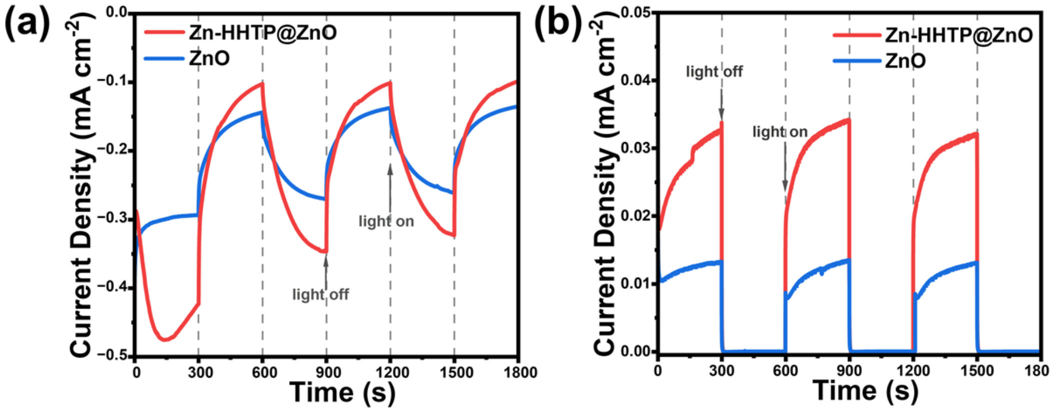

Fig. S4 (a-b) i–t curve of Zn-HHTP@ZnO and ZnO cathodes under chopped light at 2.6 and 3.0 V in 1 M lithium bis imide in tetraethylene glycol dimethyl ethe

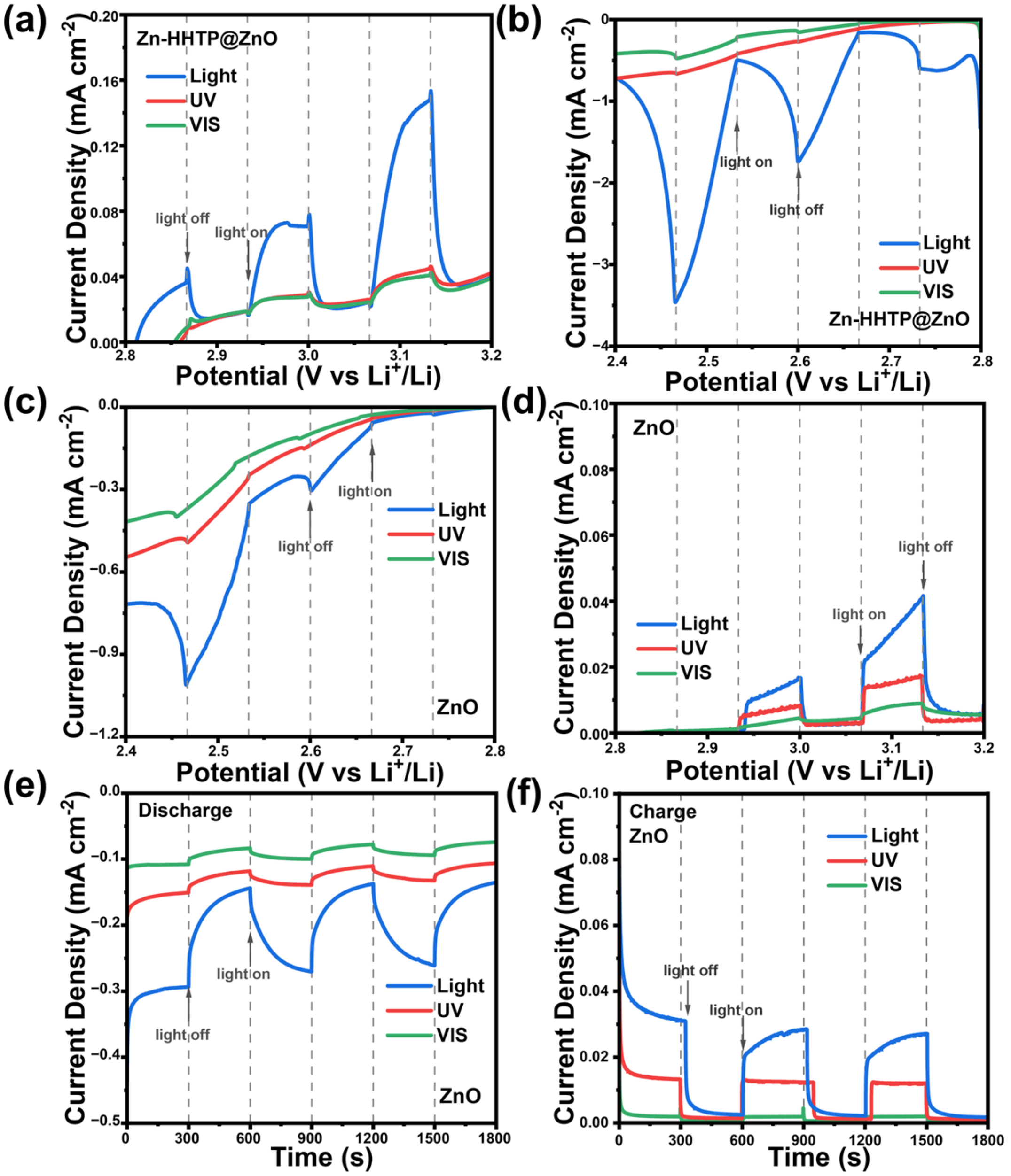

Fig. S5. (a-d) LSV diagram of Zn-HHTP@ZnO and ZnO cathodes under chopped light in different light conditions (UV, Vis and full spectrum); (e-f) i–t curves of ZnO under chopped light at 2.6 and 3.0 V in different light conditions.

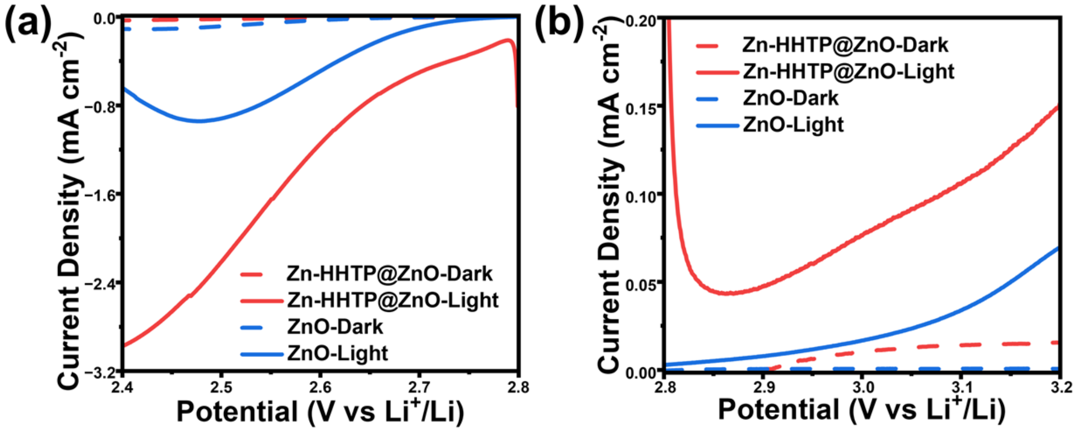

Fig. S6. (a-b) LSV curves of Zn-HHTP@ZnO and ZnO cathodes during charging and discharging under light/dark conditions.

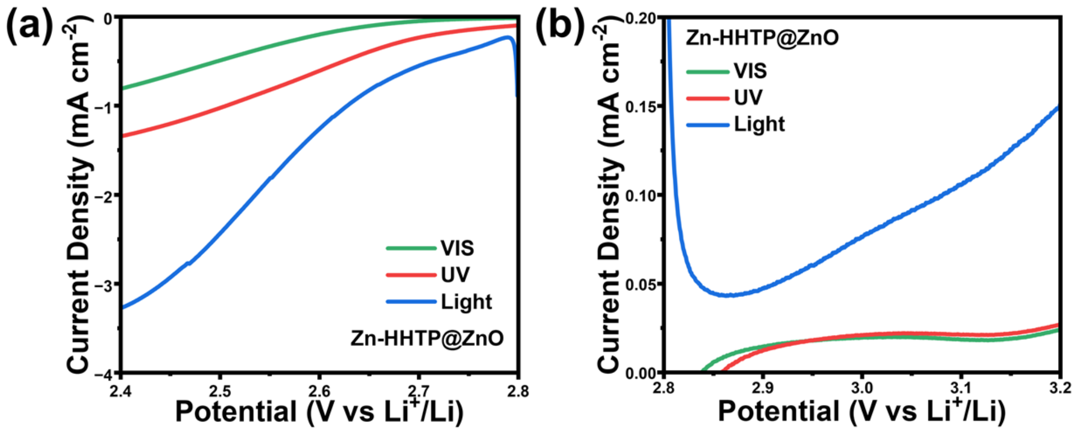

Fig. S7. (a-b) LSV curves of Zn-HHTP@ZnO cathode during charging and discharging under different spectra (UV, Vis and full spectrum).

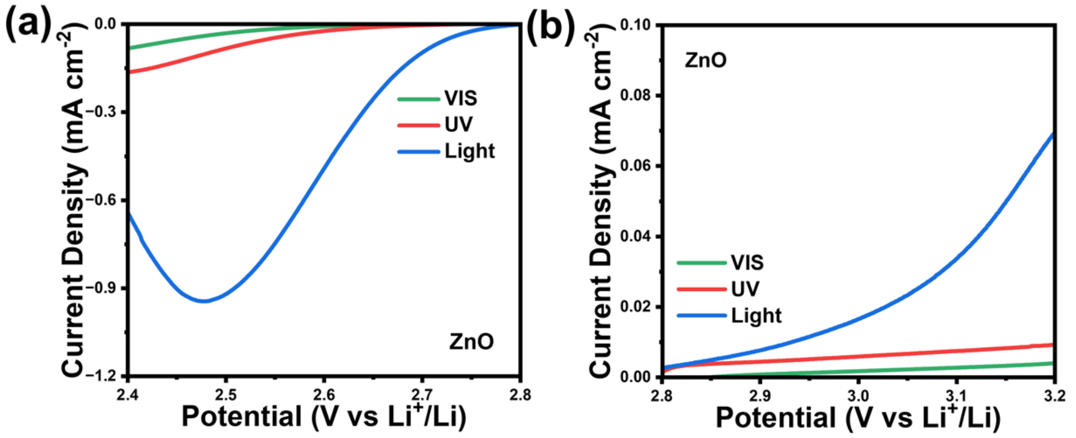

Fig. S8 (a-b) LSV curves of ZnO cathode during charging and discharging under different spectra (UV, Vis and full spectrum).

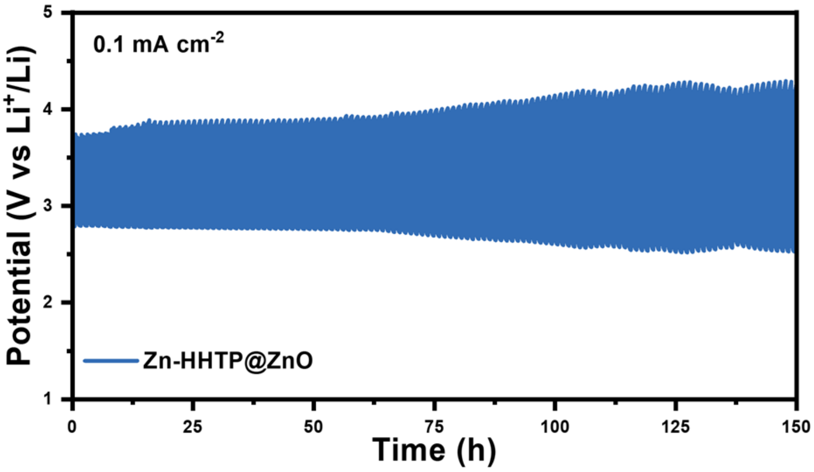

Fig. S9 The cycling performance of the Zn-HHTP@ZnO cathode under light illumination at current densities of 0.1 mA cm^{-2}

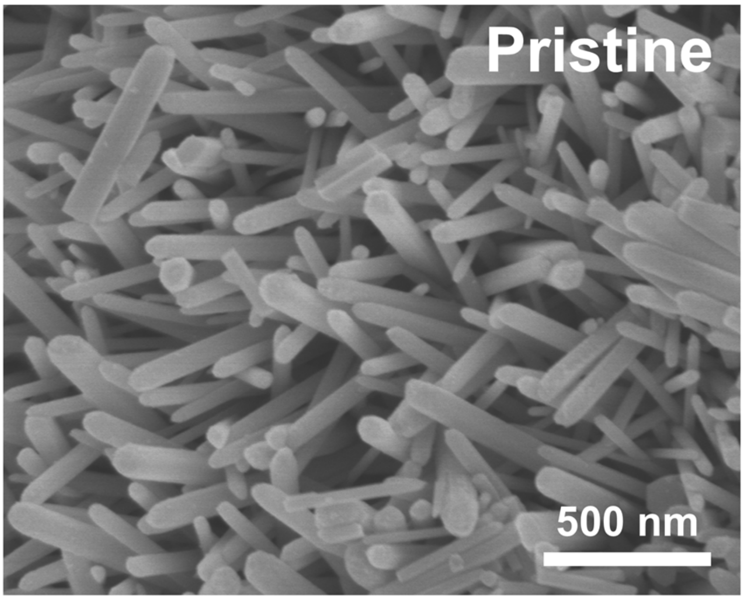

Fig. S10 SEM images of Zn-HHTP electrodes.

Table S1 Comparison of key performances between Zn-HHTP@ZnO and reported materials for enhancing ZnO's light absorption capacity.

Material Name	Visible-Light Absorption Wavelength (nm)	Band Gap Value (eV)	Ref.
Zn-HHTP@ZnO	**＞800**	**2.75**	**This work**
La/ZnO	~600	2.92	Advanced Powder Materials 1 (2022) 100004
ZnO/C	~800	3.12	Journal of Colloid and Interface Science 648 (2023) 535–550
ZnO/Fe_2O_3	~500	3.21	Ceramics International 50 (2024) 39278–39284
ZnO NCs	~760	3.36	Nano Research, 2025, 18, 94907403.
Fe-ZnOPN	~600	2.91	Rare Met. (2024) 43(11):5905–5920

Note: All of the above electrochemical data were obtained directly from the literatures or converted/evaluated based on the given electrochemical performances.

Table S2 Comparison of the electrochemical performances of Zn-HHTP@ZnO with reported cathode materials for Li-O_2 batteries.

Cathode	Discharge Voltage (V)	Charge Voltage (V)	Current Density (mA cm^{-2})	Energy Efficiency	Ref.
Zn-HHTP@ZnO	**3.0**	**3.2**	**0.02**	**93.4%**	**This work**
$CsPbBr_3$@PCN-333	3.19 ~2.6	3.44 ~3.7	0.01 0.2	92.7% 70.2%	J. Am. Chem. Soc. 2021,143,14253.
Fe_2O_3	2.68 2.56	3.09 3.15	0.06 0.12	86.7% 81.2%	Energy Storage Mater. 2020, 31, 11.
$CeVO_4$@CNT	~3 ~2.98	3.45 ~3.8	0.1 0.15	86.9% 78.4%	Nano Energy 2021, 85, 105966.
TiO_2	2.65	2.86	0.01	92%	Energy Storage Mater. 2018, 13, 49.
ZnS	2.47	2.08	0.026	>100%	Energy Storage Mater. 2018, 11, 170.
g-C_3N_4, I_2/I_3^-	2.7	1.9	0.01	>100%	Energy Environ. Sci. 2015, 8, 2664.
Au-SnO_2	3.10	3.59	100 mA g^{-1}	86.3%	New J. Chem., 2021, 10.1039/D1NJ04097A

Note: All of the above electrochemical data were obtained directly from the literatures or converted/evaluated based on the given electrochemical performances.